AD_____

Award Number: DAMD17-01-1-0435

TITLE: Optimization of Breast Cancer Treatment by Dynamic Intensity Modulated Electron Radiotherapy

PRINCIPAL INVESTIGATOR: David K. Gaffney, M.D., Ph.D.
Dennis D. Leavitt, Ph.D.

CONTRACTING ORGANIZATION: University of Utah
Salt Lake City, UT 84132

REPORT DATE: April 2006

TYPE OF REPORT: Final

PREPARED FOR: U.S. Army Medical Research and Materiel Command
Fort Detrick, Maryland 21702-5012

REPORT DOCUMENTATION PAGE

Form Approved
OMB No. 0704-0188

1. REPORT DATE	2. REPORT TYPE	3. DATES COVERED
01-04-2006	Final	1 Oct 2001 – 31 Mar 2006

4. TITLE AND SUBTITLE

Optimization of Breast Cancer Treatment by Dynamic Intensity Modulated Electron Radiotherapy

5a. CONTRACT NUMBER

5b. GRANT NUMBER
DAMD17-01-1-0435

5c. PROGRAM ELEMENT NUMBER

6. AUTHOR(S)

David K. Gaffney, M.D., Ph.D.
Dennis D. Leavitt, Ph.D.

Email: dennis.leavitt@intermountainmail.org

5d. PROJECT NUMBER

5e. TASK NUMBER

5f. WORK UNIT NUMBER

7. PERFORMING ORGANIZATION NAME(S) AND ADDRESS(ES)

University of Utah
Salt Lake City, UT 84132

8. PERFORMING ORGANIZATION REPORT NUMBER

9. SPONSORING / MONITORING AGENCY NAME(S) AND ADDRESS(ES)
U.S. Army Medical Research and Materiel Command
Fort Detrick, Maryland 21702-5012

10. SPONSOR/MONITOR'S ACRONYM(S)

11. SPONSOR/MONITOR'S REPORT NUMBER(S)

12. DISTRIBUTION / AVAILABILITY STATEMENT
Approved for Public Release; Distribution Unlimited

13. SUPPLEMENTARY NOTES

14. ABSTRACT

This project clearly demonstrates that intensity modulated electron arc radiotherapy is feasible using the photon multi-leaf collimator of a modern linear accelerator. Secondary and tertiary collimators are replaced by the multi-leaf collimator and by dynamic field edge enhancement. Three-dimensional dose calculation models are required in order to properly account for changing patient shape both axially and in the cephalo-caudal direction. Both Monte Carlo and 3-dimensional pencil beam algorithms have been examined. Comparison of electron arc therapy dose distributions vs. standard photon tangent breast fields show that a more uniform dose distribution is achievable by dynamic electron arc, match-line inhomogeneities can be minimized or avoided, and dose to lung and critical organs can be reduced. Particular advantage is noted in treatment plans for bilateral post-mastectomy breast treatment. Continuing issues include 1)calculation throughput, even with up to 32 processors calculating in parallel, 2)implementation in a clinical mode readily available to radiotherapy clinics,3)automation of dynamic field edge enhancement. Further discussion with the radiotherapy vendors will be required.

15. SUBJECT TERMS
Breast Cancer

16. SECURITY CLASSIFICATION OF:			17. LIMITATION OF ABSTRACT	18. NUMBER OF PAGES	19a. NAME OF RESPONSIBLE PERSON
a. REPORT	b. ABSTRACT	c. THIS PAGE			USAMRMC
U	U	U	UU	24	19b. TELEPHONE NUMBER *(include area code)*

Table of Contents

INTRODUCTION

Subject: Electron Arc Therapy was developed to treat extended superficial volumes within the postmastectomy chest wall. Although this technique has been applied to other superficial disease sites it has remained of primary application to the postmastectomy chest wall. Primary advantages proposed for this technique include 1) reduced dose inhomogeneity at abutment sites; 2) improved dose homogeneity across the extended chest wall; 3) limitation of dose to underlying critical structures such as heart and lung; and 4) reduced dose to the apex of the lung through use of electrons rather than a photon field across this region. Limitations of this technique include 1) the extensive labor required to fabricate the secondary and tertiary field defining apertures; 2) extensive treatment planning time to calculate the electron arc dose distributions and to "optimize" the shape of the secondary aperture to deliver the desired uniform dose.

Purpose: The purpose of this work was to devise methods to overcome the above listed limitations (extensive preparatory labor of secondary and tertiary field defining apertures, and extensive treatment planning time to calculate electron arc "optimized" dose distributions), and to improve the treatment planning capability and dose delivery capability through implementation of **I**ntensity **M**odulated **E**lectron **R**adio**t**herapy **(IMERT).** Using methods similar to static field photon IMRT, IMERT defines the electron arc fields using the primary photon Multi-Leaf Collimator, adjusts the individual leaves of the MLC to define the specific field shapes required for each segment as the gantry rotates around the patient. The specific field shapes defined by the MLC leaves, and the specific dose to be delivered for each arc segment is to be determined by the optimization code.

Scope: This work represents a unique extension of treatment planning and dose delivery tools for electron radiotherapy. This is the first application of photon collimators to electron radiotherapy, and tests the capability of complex Monte Carlo dose calculation codes to compute electron arc dose distributions in a reasonable length of time. This work investigates innovations to eliminate labor-intensive fabrication of secondary and tertiary field shaping devices by using the photon MLC and a simple accessory trimmer. The end product of this work is a direct comparison of IMERT vs. standard post-mastectomy treatment techniques.

BODY

Five specific tasks were identified as part of this work:

1. Implement a 3-dimensional electron dose calculation model for the electron arc studies.
2. Measure the dose characteristics of electron beams defined by the photon MLC.
3. Confirm efficacy of 3-D dose calculations using phantoms simulating actual patient shapes.
4. Compare Dose-Volume-Histograms for target volume, heart, and lungs for IMERT vs. other chest wall radiation therapy techniques.
5. Test clinical applicability: Treatment Planning Time and Actual Treatment Time for IMERT vs. standard forward planning.

- **Dose Calculation Model:** The first attempts at dose calculations for electron arc therapy employed bilinear interpolation from measured tabular profile and central axis depth dose data. Similarly, the dependence of dose on electron arc aperture was determined from bilinear interpolation of dose vs. field width measurements. The dependence on distance superior or inferior to the central axis plane was determined by including a long-axis profile. These bilinear interpolation techniques allowed a relatively fast calculation, enabling iterative adjustments of aperture shape followed by a repeat calculation with the modified aperture. These were gross calculations that did not account for step-wise change in the aperture shape as the individual leaves of the photon Multi-Leaf Collimator (MLC) were adjusted.

The introduction of the more sophisticated three-dimensional calculation techniques, namely the electron pencil beam algorithm and electron Monte Carlo calculation, enabled a more realistic calculation of dose for field shapes determined by the MLC. However, the tradeoff was extended calculation times for both models. We attempted to reduce the calculation time by ganging twenty to twenty-five PC's with CPU speeds from 2.0 to 2.8 GHz, thereby simultaneously calculating dose contributions for twenty to twenty-five arc segments. Unfortunately, the overhead for these calculations was excessive, and we were unable to get calculation times reduced commensurate with the number of PC's thrown into the calculations. In order to be viable in an interactive mode, a more efficient way to parse the tasks to this set of waiting computers must be found. For the electron Monte Carlo calculations, a description of the entire electron beam line, starting with the vacuum window and extending through the patient, was provided (Figure 1). Using this complete description, the electron dose profiles, central axis depth doses, and relative output were correctly calculated by the electron Monte Carlo code (Figures 2-5). The effect of the rounded ends of the photon MLC was correctly modeled. These studies clearly demonstrated that the electron Monte Carlo code could provide accurate representation of the electron arc doses. However, the calculation time remains inordinate, thereby seriously compromising the efficacy of the Monte Carlo technique.

Coincident with the former Principal Investigator's move to Intermountain Health Care, a new array of computers was purchased and installed at LDS Hospital. All dose calculations were moved to this system, and the array at the University of Utah was dismantled and reassigned to other tasks. Although the CPU's were marginally faster, the limiting factor remained the overhead of assigning the tasks to the individual computer boxes.

A suggestion that is yet to be incorporated into the calculation is to model the effects of all components upstream of the MLC using either an analytic model or pre-calculated data tables. Additionally, intuitive adjustments of the electron interaction parameters within the MLC, such as depth beyond which no calculations within the MLC would be required, were not implemented. These and other refinements of the code process could be applied to improve the overall performance. If conditions allow, a commercial electron Monte Carlo code will be applied to the electron arc therapy problem. This code treats everything upstream of the field-shaping aperture as an analytic function, thereby achieving significant savings in calculation time. Additionally, if successfully implemented, this code could serve as the backbone of a commercial treatment-planning package for electron arc therapy.

- **MLC-defined Electron Beams:** The two primary differences in the beam-line for the MLC-defined vs. the secondary-aperture-defined electron profiles are 1) the distance of the MLC or aperture from isocenter; and 2) the rounded (MLC) vs. straight (Cerrobend) field-defining edge. The MLC is positioned 50 cm upstream from isocenter and is 5 cm thick with the rounded field defining edge. This introduces a greater wide-angle scatter component; the 50 cm of air from the MLC to isocenter also introduces additional air scatter leading to a wider beam profile. By comparison the Cerrobend aperture is approximately 1.5 cm thick, has straight edges, and is located in the accessory tray holder at a distance of only 35 cm from isocenter. Thus, for the same light field projection at isocenter, the electron field defined by the MLC is wider than the electron field defined by the Cerrobend aperture. The diffuse nature of the beam profiles is more pronounced at the lower electron energies. As the electron energy is increased, the electron scattering from the collimator (either MLC or Cerrobend aperture) is directed more in the forward direction. The attached illustrations show a comparison of the MLC-defined profiles vs. the Cerrobend aperture-defined profiles (Figures 5,6). The net effect regarding our efforts to remove the tertiary cast from the preparation phase is that the penumbra at the field edge will be slightly larger than that produced using the Cerrobend aperture. This marginal increase in field-edge penumbra

is judged to be acceptable. Therefore, the challenge to remove the secondary aperture and the tertiary patient cast has been met. We have demonstrated that the required field shapes can be defined using the MLC and that the tertiary patient casting can be deleted from the planning techniques and the treatment delivery.

Efficient determination of the optimized field shape for each arc increment remains a difficult problem. The new Millennium MLC has 60 leaf pairs. Unconstrained searches treating each leaf pair as an independent variable were unstable and did not produce consistent field shapes. To stabilize the searching, we introduced three pivot points superior to the central axis and three inferior, and required the individual leaf pairs to move to the line connecting the pivot points. This reduced the search gradients to seven independent points. The resulting field shapes are illustrated in Figure 7. The reference dose map shown in Figure 8 demonstrates that we are not yet able to get complete agreement of desired vs. actual dose across the entire chest wall. The greatest deviation occurs at the extreme of the sloping chest wall where the effects of oblique incidence are greatest (see next section, efficacy of 3-D dose calculations).

- **Efficacy of 3-D Dose Calculations:** Tabular and 2-dimensional dose calculations are limited by the assumption that the patient contour remains the same in planes superior or inferior to the calculation plane. There is no correction for scatter differences resulting from patient contour changes superior-to-inferior. The known effects of oblique incidence of the electron beam, i.e., changing patient contour superior-to-inferior, are 1) decrease in the depth of maximum dose; and 2) departure from simple inverse-square distance correction for dose. These effects are explicitly included in the three-dimensional dose calculations. In the series of images in Figure 7, an axial CT, complete with arc angle segment illustrated, is displayed to the left; a sagittal reconstruction of the patient contour corresponding to this arc angle segment is displayed to the right, and the MLC field shape is superimposed for each arc angle segment. These images reveal that there is a significant reduction in thorax thickness as planes superior to the central axis are considered for calculation. The electrons incident on the chest through this beam angle are therefore incident obliquely on the chest. This introduces the undesired effect of moving the depth of maximum dose to a shallower level, thereby potentially under-treating the deeper volume. Before the introduction of Multi-leaf Collimators, we treated chest wall patients in the supine position, with the patient's back flat onto the treatment couch table. This was done in order to minimize the divergence of the supraclavicular photon field into the underlying lung. With the introduction of MLC's, setting the central axis to the superior edge of the electron arc field and closing the inferior jaw can minimize photon field divergence and MLC leaves to the central axis. Now the sloping chest wall anatomy can be modified by inserting a support wedge beneath the patient, thereby adjusting the anterior surface of the thorax into a more level topography. In this circumstance, the depth of maximum dose in the superior planes will remain more constant. This illustration demonstrates the importance of reliable dose computation models: the simpler two-dimensional tabular and pencil beam models completely miss the dramatic modification of the dose distribution due to oblique field entry, while the three-dimensional models correctly calculate this effect.

The effect of oblique incidence of the electron field onto the chest wall is illustrated in Figure 9 where the dose distributions in the central axis plane and planes 4 cm and 8 cm superior and inferior are compared. The three-dimensional dose calculations clearly show the reduction in depth of dmax. This demonstrates one significant advantage of the three-dimensional dose calculations compared to the simpler two-dimensional tabular or pencil beam calculations.

- **Comparison of IMERT Arc vs. Standard Treatment Technique:** The bilateral post-mastectomy chest wall presents difficult radiation therapy treatment planning and dose delivery problems. As shown in figure 10, the surface area to be treated is extensive, and the presence of underlying critical lung

structure requires that effort be made to protect these structures. Typically, two sets of parallel-opposed tangent photon fields would be applied, and the beams would be adjusted to minimize the "gap" or the "overlap" at the junction between the two sets of fields. The net effect of this treatment setup is to treat to a different depth across the chest wall, according to the placement of the photon fields; and to accept a triangular shaped region of reduced dose immediately below the field junctions. By applying electron arc to this case, the entire curving chest wall can be treated to the same depth, the hot-spot/cold-spot at the junction of the photon fields is avoided, and dose to the underlying lungs and heart is minimized (Figure 11). The attached isodose distributions and Dose-Volume-Histograms (DVH) (Figure 12) demonstrate this.

A significant key to minimizing dose to the underlying lung is to create a patient-specific range-limiting bolus that fits over the patient chest wall and adds an effective depth of tissue-equivalent material so that at least a minimum thickness can be maintained across the entire chest wall. Using this technique, a specified isodose line can be conformed to the lung-chestwall interface. This is illustrated in the comparison of the same bilateral electron arc with/without added bolus.

Nearly as challenging is the single-sided post-mastectomy chest wall treatment. If internal mammary nodes are positive, the radiation fields must include both the involved left or right chest wall and the internal mammary chain. If not, the treated volume can be contained within a pair of "shallow" photon tangents; if internal mammary nodes are positive, the volume can be treated using "deep" photon tangents that encompass the Internal Mammary Chain but also include a greater fraction of the lung volume within the treatment field. Alternatively, the volume can be treated using a "shallow" photon tangent pair supplemented by an electron field covering the internal mammary nodes. This electron field can be set up either directly perpendicular to the Internal Mammary Chain, or can be angled coincident to the central axis of the photon field. The primary drawback of the deep photon tangent treatment is that the heart and lung are included in the tangent photon field, and thereby receive a significant dose from the tangent fields. The primary drawback of the tangent photon plus IMC electron field is the dose inhomogeneity at the junction of the electron and the photon tangent fields. Conversely, the two primary advantages of the electron arc application are 1) uniform dose across the entire chest wall, including a deeper treatment depth through the Internal Mammary Chain; and 2) minimization of dose to the underlying lung and heart. These combinations are demonstrated in the attached illustrations.

- **Comparison of Treatment Planning Time and Treatment Delivery Time:** As noted above, electron techniques offer significant advantage in dose uniformity and normal organ dose sparing compared to standard photon techniques. However, electron arc treatment planning and dose delivery are more time consuming than standard tangent photon planning and delivery. First, the electron dose calculation per field takes longer; second, the electron arc is calculated as the sum of a series of fixed electron fields; and third, the electron arc treatment is delivered as a sequence of smaller arc segments. For example, a typical electron arc of 120 degrees will be delivered as a sequence of 12 arcs of 10 degrees each. The MLC is set to a fixed shape for each arc sequence. To update the MLC for the next segment, the next field must be programmed. The MLC shape is read from a file and the individual leaves move to the correct position for that segment. The required dose is set and the program cycle is completed. This process is repeated 12 times for this arc. The process required to program the next arc segment parameters into the treatment console is not yet automated, so it must be repeated manually for each arc segment. This adds significant overhead to the dose delivery process for electron arc therapy.

1) Photon field dose calculation time (per field): __ 20"_____
   Electron field dose calculation time (per field): __ 11'_____

2) Electron arc dose calculation time (60 fields/120 degree arc): _ 31’_____
(32 processors calculating; so if this were done on a single processor using this code it would require approximately 16 ½ hours calculation time. Simple scaling of the 11’ calculation time per field for a single processor would suggest that the time when using 32 processors could be as little as 22 minutes; however, some of the initial parameter setup for each field is done at the front end, before the fields are parsed out to the individual computers. This could be investigated as a potential roadblock that can be minimized.)

3) Tangent Photon opposed field dose delivery (Linac):
   a) Program first field & Rotate Gantry __30”_____
   b) Deliver Dose __20”_____
   c) Program Second Field & Rotate Gantry __30”_____
   d) Deliver Dose __20”_____
   e) TOTAL TIME __1’40”_____

4) Electron Arc dose delivery (120 degree arc/1 segment):
   a) Program first arc segment __30”_____
   b) Deliver Dose __73”_____
   b) TOTAL TIME __1’43”_____

5) Electron Arc dose delivery (120 degree arc/12 segments):
   a) Program first arc segment __25”_____
   b) Deliver Dose ___5”_____
   c) Program Second Arc Segment __25”_____
   d) Deliver Dose ___5”_____
   ……..
   e) Program Last Arc Segment __25”_____
   f) Deliver Dose ___5”_____
   g) TOTAL TIME __6’_____

Comparing the two arcs, it is clear that the overhead for multiple arc segments is the setup and programming time for each segment. The total “beam-on” time remains the same. Thus, the overhead for a 12-segment arc is approximately 10 ½ minutes of the total 12 minute delivery time. This overhead could be removed or dramatically reduced if the manufacturer would provide the tools to combine several arc segments without the necessity to reprogram between each segment. This capability is available for standard treatment techniques, so it may be an option that can be developed with little expense to the manufacturer.

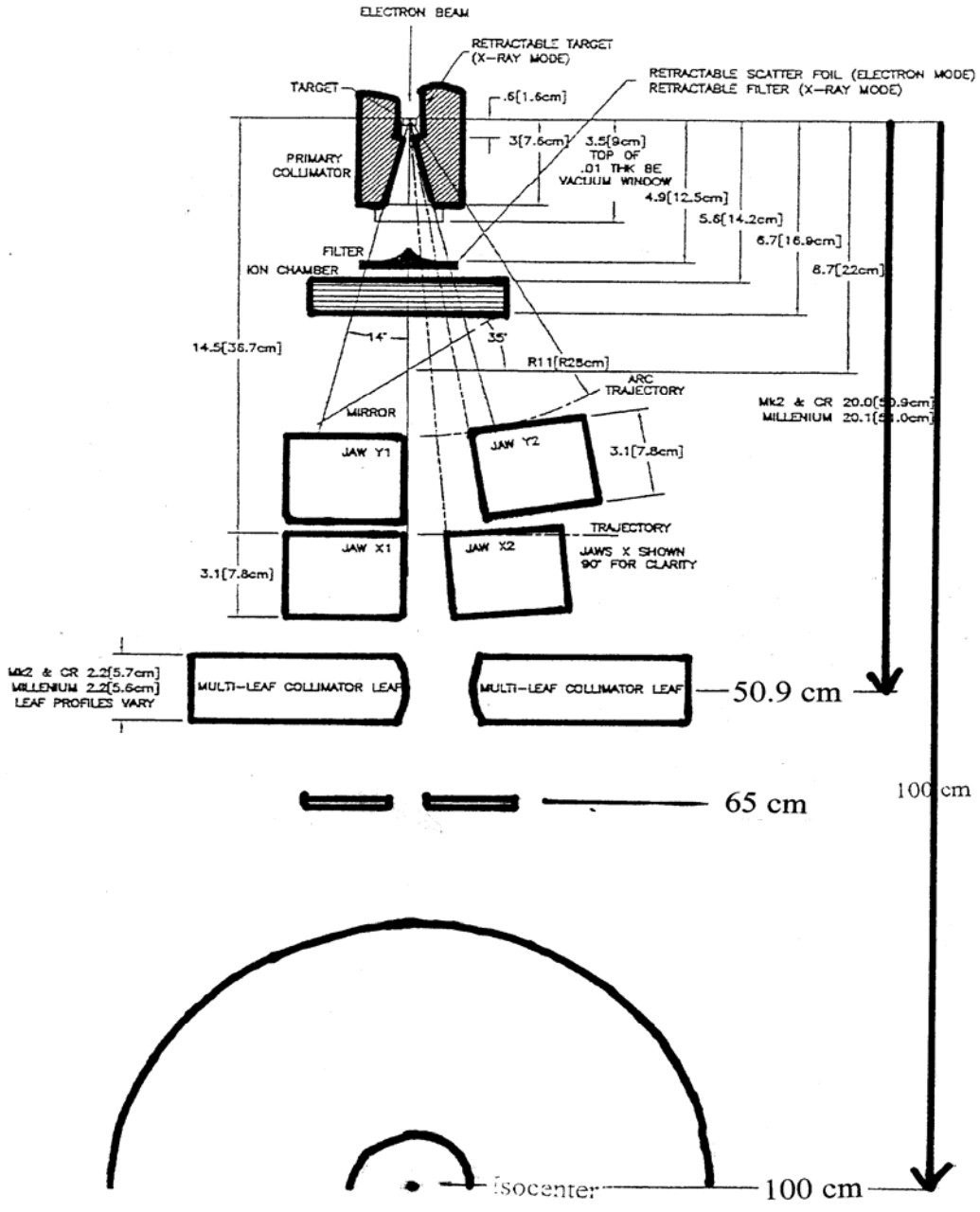

Figure 1: Schematic diagram of electron beamline showing location of scattering foil, ionization chamber, primary photon jaws, Multi-leaf collimator and secondary Cerrobend aperture. In the electron application, the "target" is withdrawn from the electron beam and replaced with a scattering foil, and the primary photon jaws are fixed to a specified field size such as 10 cm wide by 40 cm long. The Multi-leaf collimator then accomplishes Field shaping. When the MLC is used for field definition, the Cerrobend aperture is completely removed from the beam. The two semicircles represent the extremes of phantom sizes used for electron arc therapy dosimetry studies.

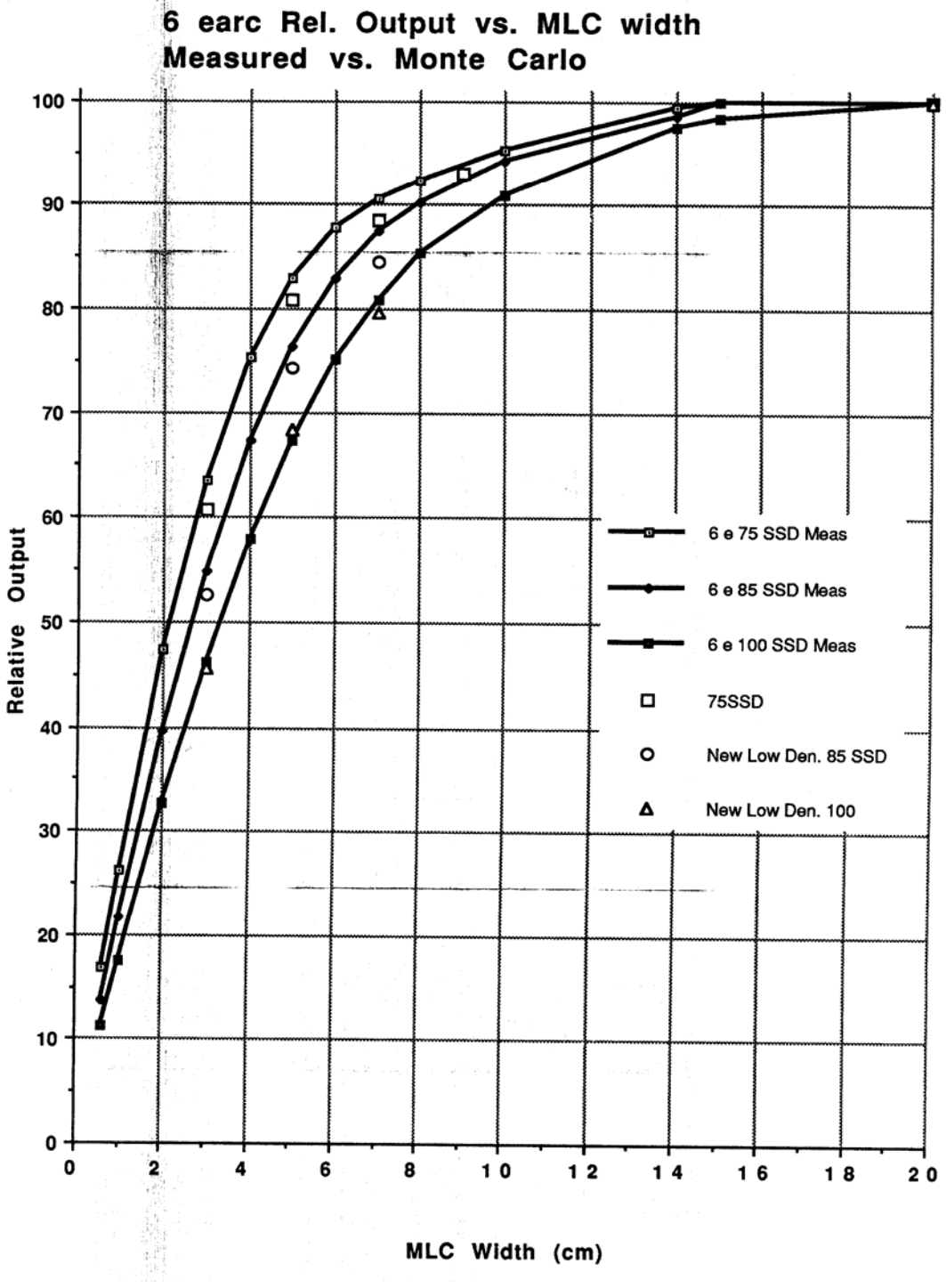

Figure 2: Graph of relative output vs. MLC width for SSD's of 75 cm, 85 cm and 100 cm. Data are normalized to output for primary photon jaws set to 20 cm x 40 cm. Measurements were made in phantom at depth of maximum dose. The Monte Carlo dose calculations explicitly include density correction for air scatter and absorption. The calculations using air density 15% less than at sea level produce excellent agreement with measurement at 4500 feet altitude.. These curves illustrate that increasing or decreasing the field width applied to the arc electrons easily achieves dose adjustment.

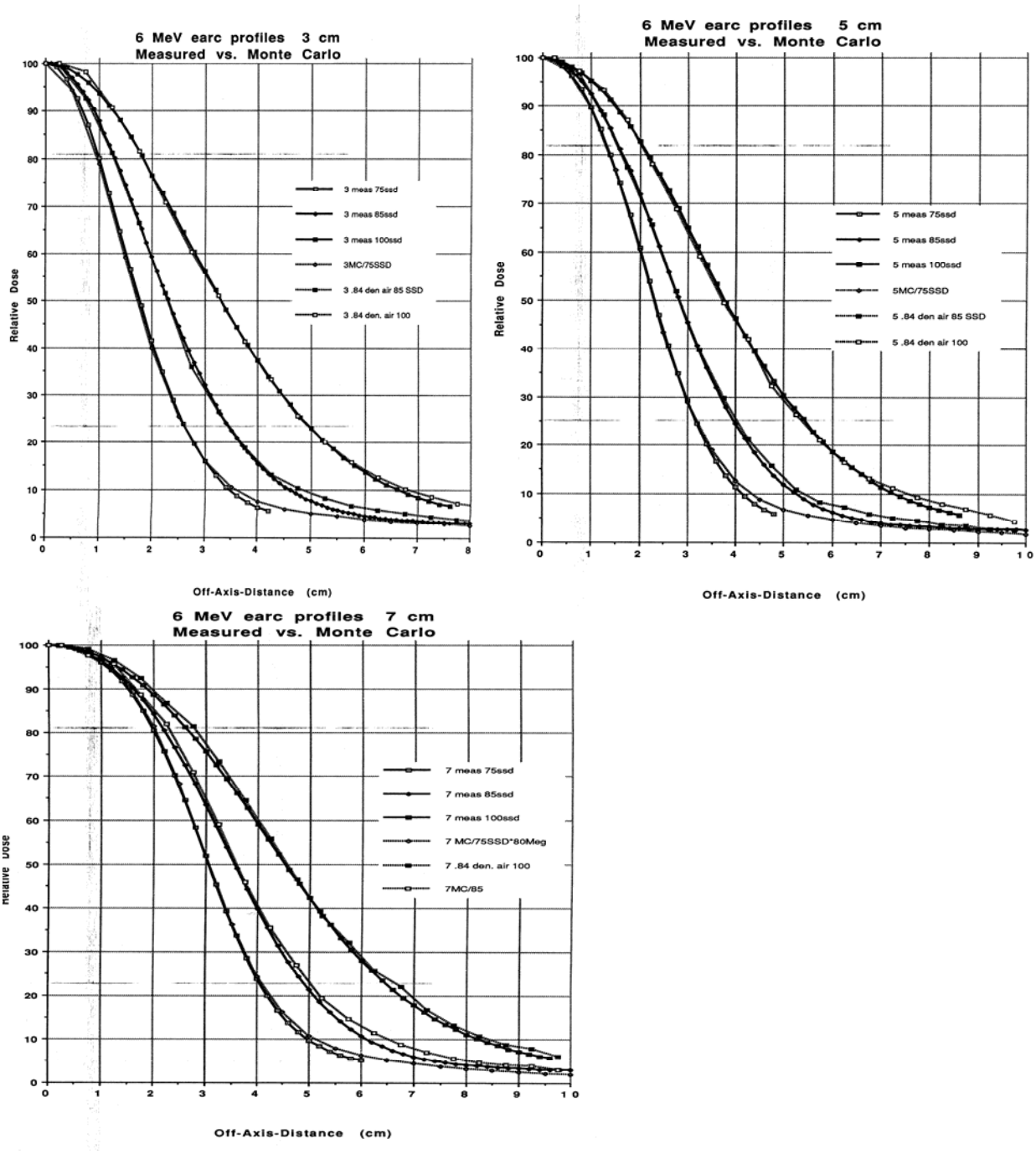

Figure 3: Comparison of measured vs. Monte Carlo calculated electron arc beam profiles. Profiles are displayed for three different field widths, 3 cm, 5 cm, and 7 cm corresponding to the range of field widths applied clinically. Profiles are displayed for three SSD's of 75 cm, 85 cm and 100 cm corresponding to the range of SSD's employed clinically. When the effects of less dense air at Utah altitude are included, the measured and calculated beam profiles are in excellent agreement. This is validation of the correct use of the Monte Carlo calculation code.

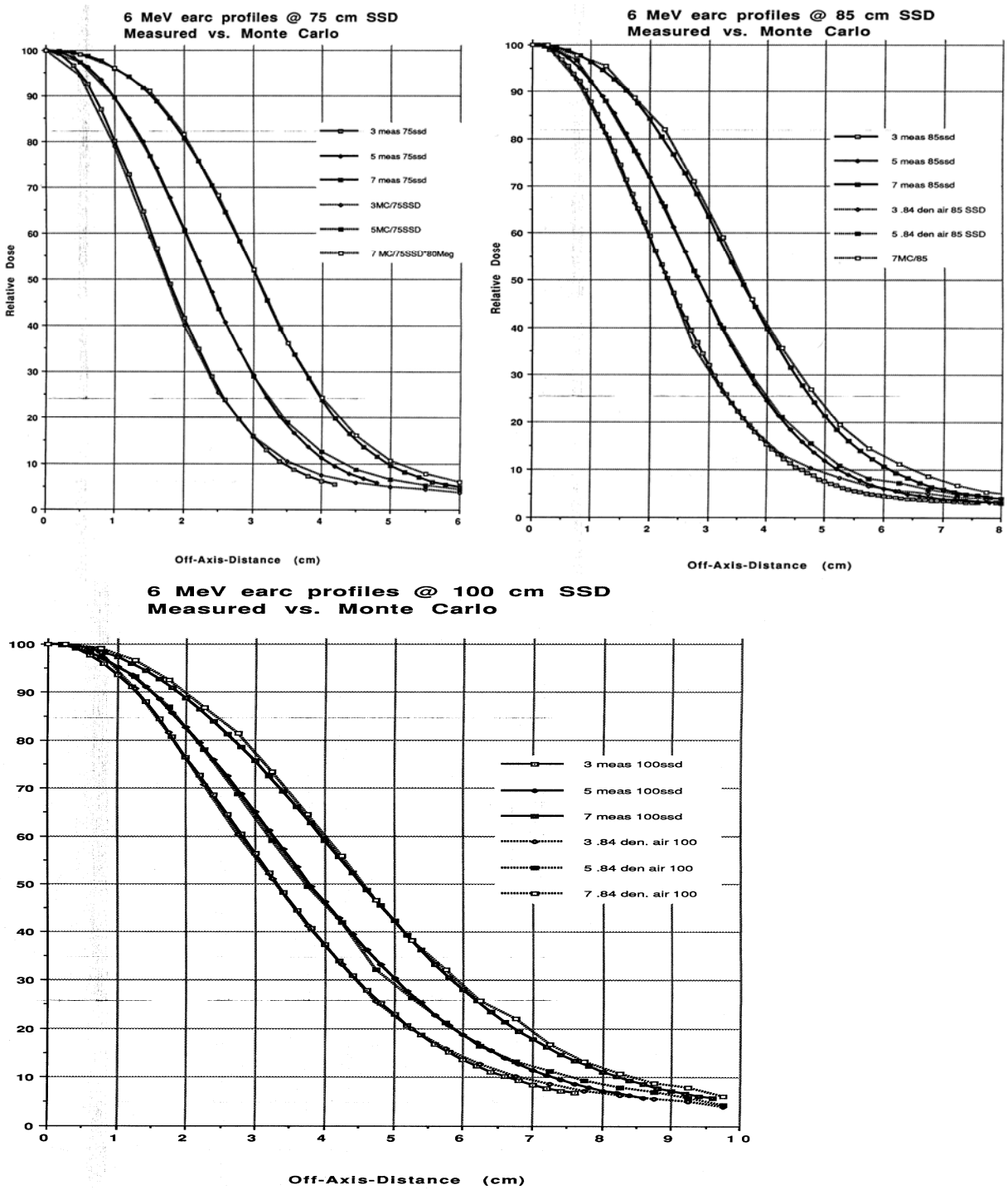

Figure 4: Measured vs. calculated beam profiles are displayed for field widths of 3 cm, 5 cm and 7 cm. The three graphs represent the data at SSD's of 75 cm, 85 cm and 100 cm.

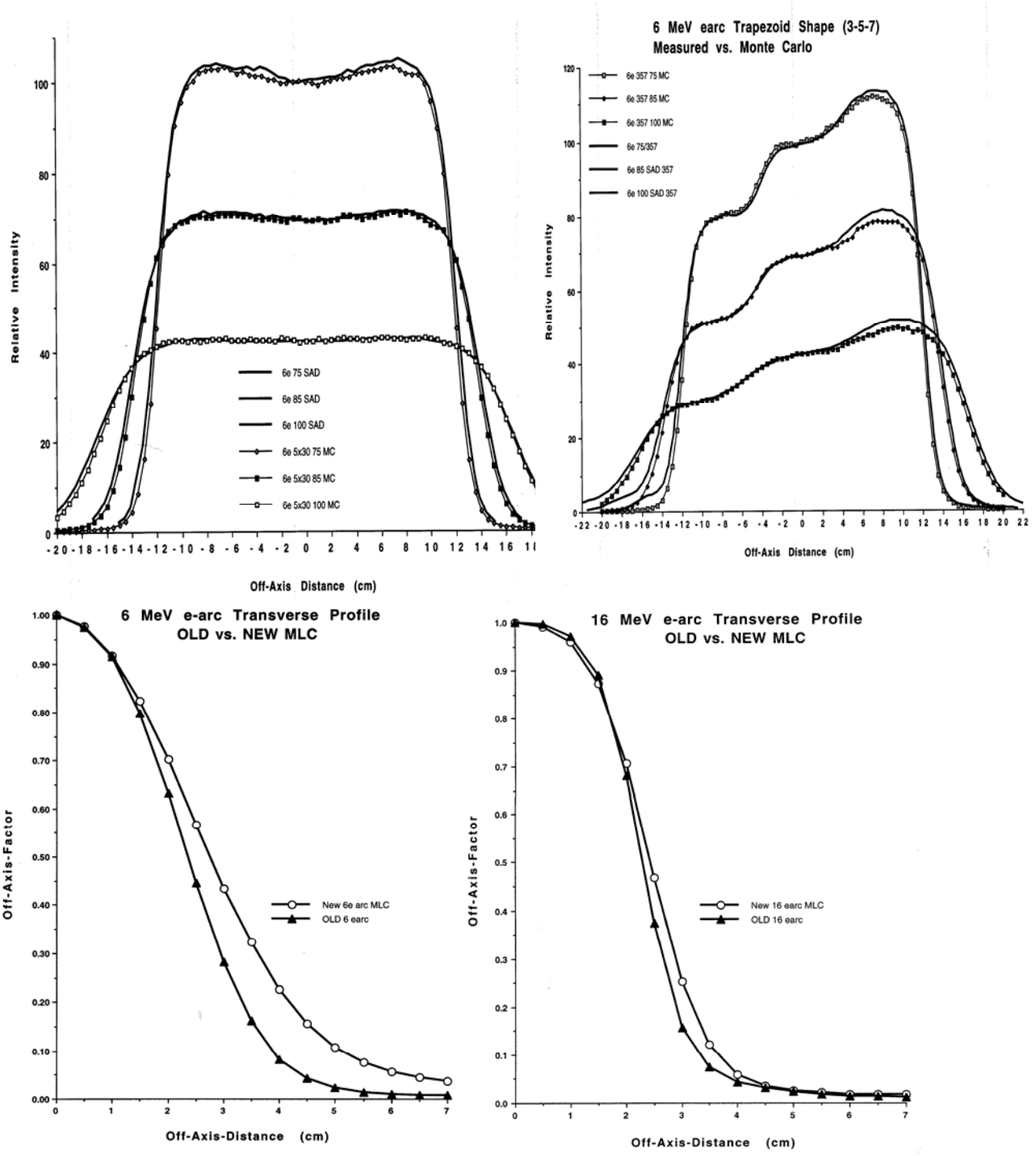

Figure 5: Upper Left: Long-axis profile measured vs. calculated at 75 cm, 85 cm and 100 cm for rectangular field. Upper Right: Long-axis profile measured vs. calculated at 75, 85 and 100 cm for trapezoidal shaped field consisting of three segments 2 cm, 5 cm and 7 cm wide. Bottom Left: Comparison of transverse profile for MLC vs. Cerrobend aperture. The Cerrobend aperture produces the sharpest beam profile, since the aperture is 15 cm closer to the phantom. Bottom Right: comparison of transverse profile for MLC vs. Cerrobend aperture using 16 MeV electrons. Since the higher energy electrons are scattered in a more forward direction than were the 6 MeV electrons, the difference between the MLC and Cerrobend profiles is less than for 6 MeV electrons.

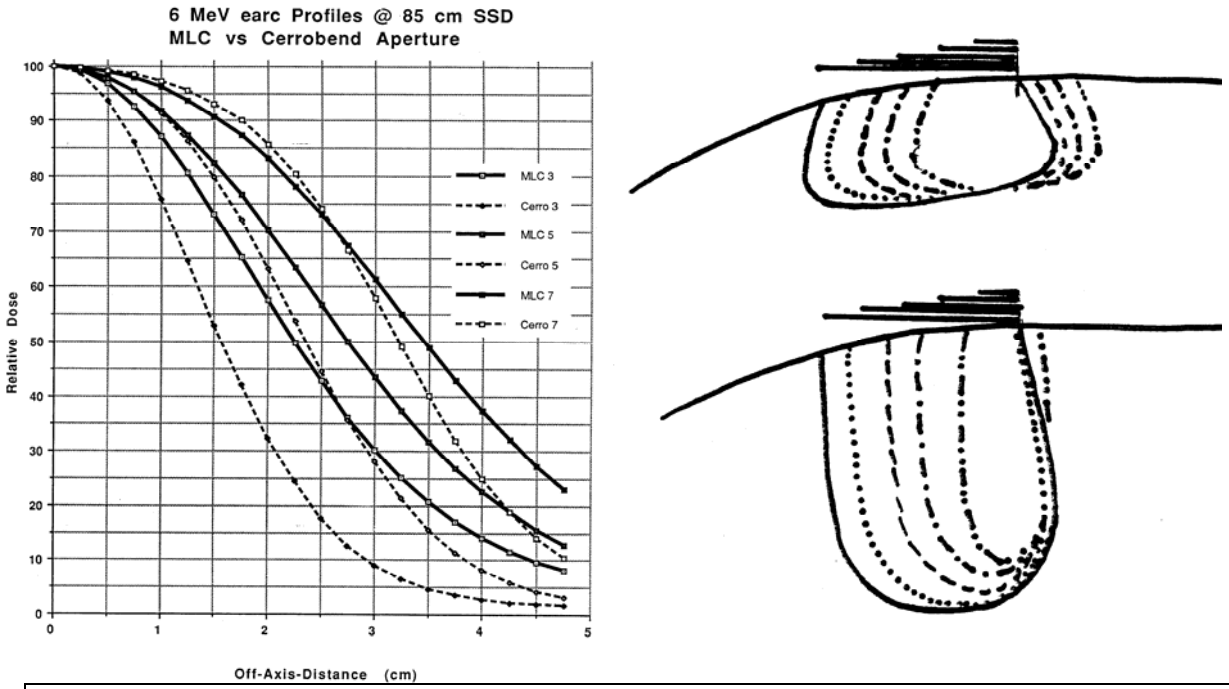

Figure 6: Upper Left: Comparison of electron beam profiles for MLC vs. Cerrobend aperture for 3, 5 and 7 cm wide projected fields. Upper Right: Comparison of reduced width fields applied at end of arc to create sharp field edge. The reduced fields for 6 MeV are wider than for 16 MeV due to the increased lateral scatter of the 6 MeV electrons. Because of this, the field edge for 6 MeV arc distribution is not as abrupt as with tertiary collimation. However, as the electron energy increases the field edge sharpness improves, finally exceeding that of tertiary collimation.

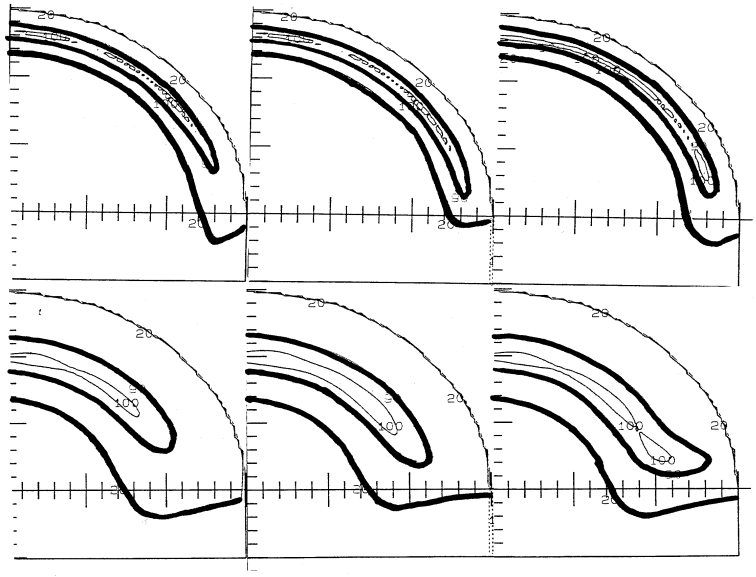

Upper three frames: 6 MeV Isodose distribution at end of arc comparing no Cerrobend shielding at desired edge of field (left); Cerrobend shielding at desired edge of field (middle); and field edge definition using sequentially narrower fields to build up dose at desired field edge. Lower three frames: 16 MeV isodose distributions for same three dose techniques.

Figure 7: The left panel shows the axial CT through central plane and highlights the arc segment of interest. The right panel shows the shape of the MLC for this arc segment and shows the sloping chest wall onto which the electron field for this segment is incident. These views are with the patient supine on the flat couch.

A vertical yellow line has been added to emphasize the departure of the sloping chest wall from a simple flat surface. The greatest departure is seen in the superior planes. In future treatments, the patient would be angled upward off the straight surface to minimize the chest slope.

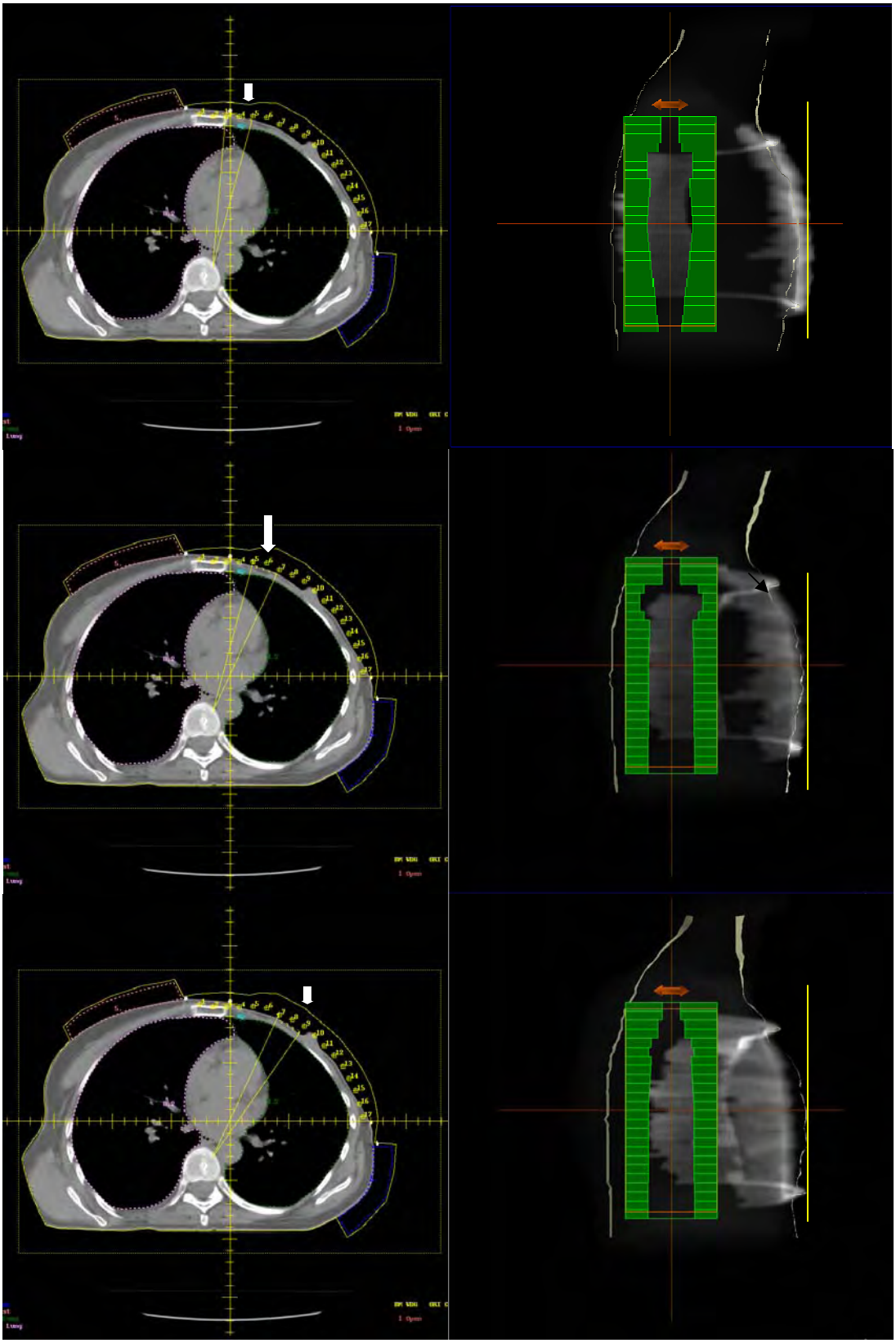

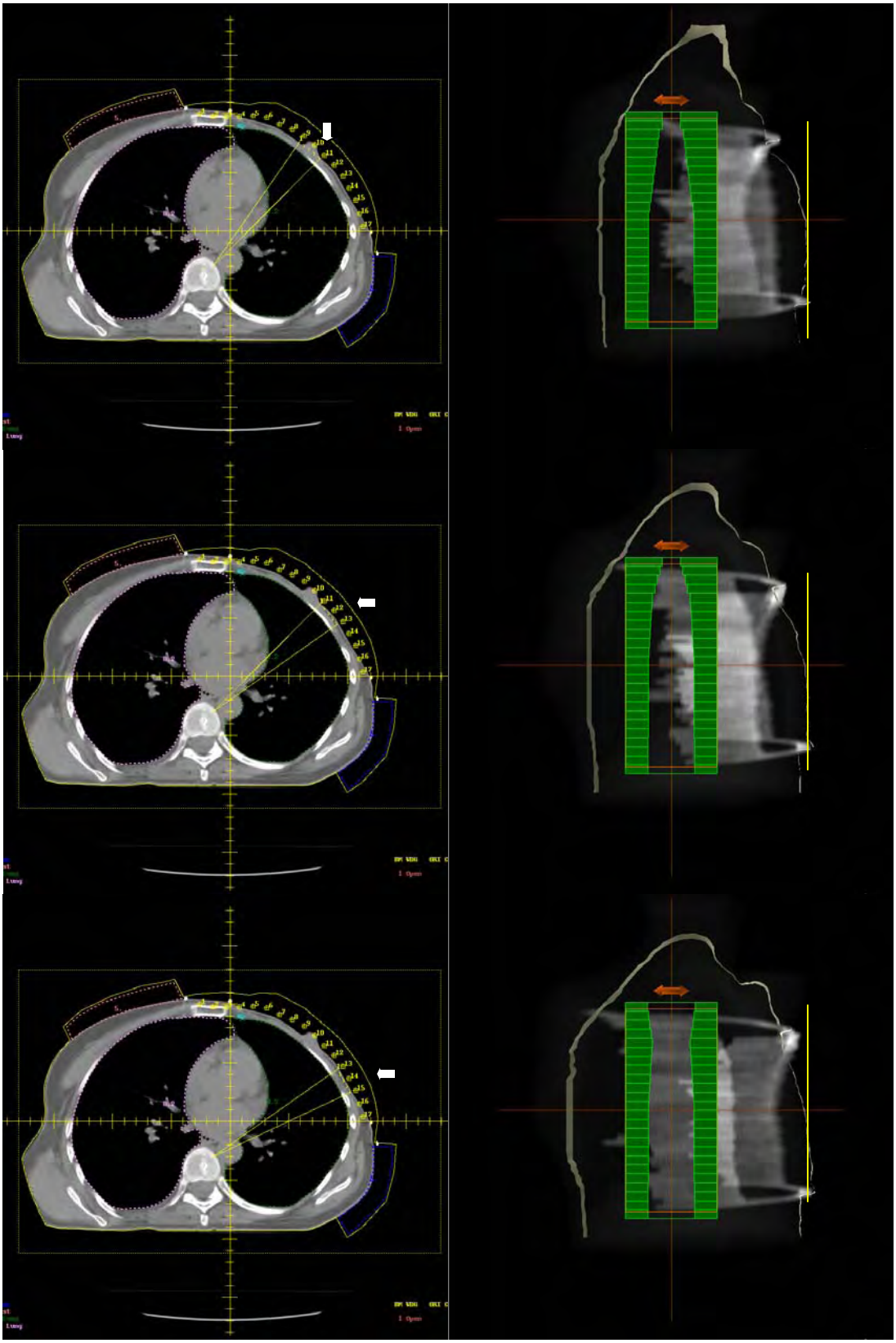

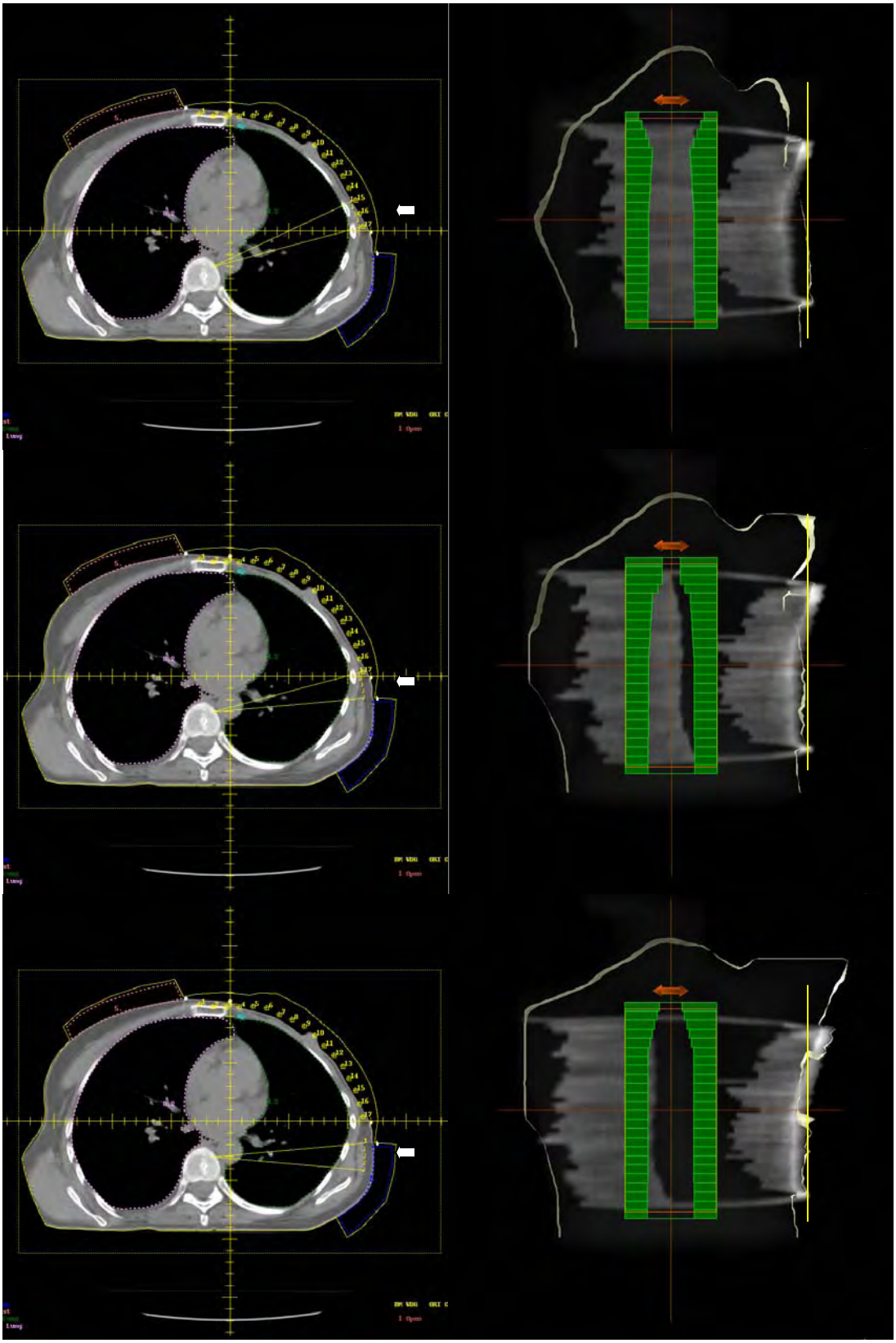

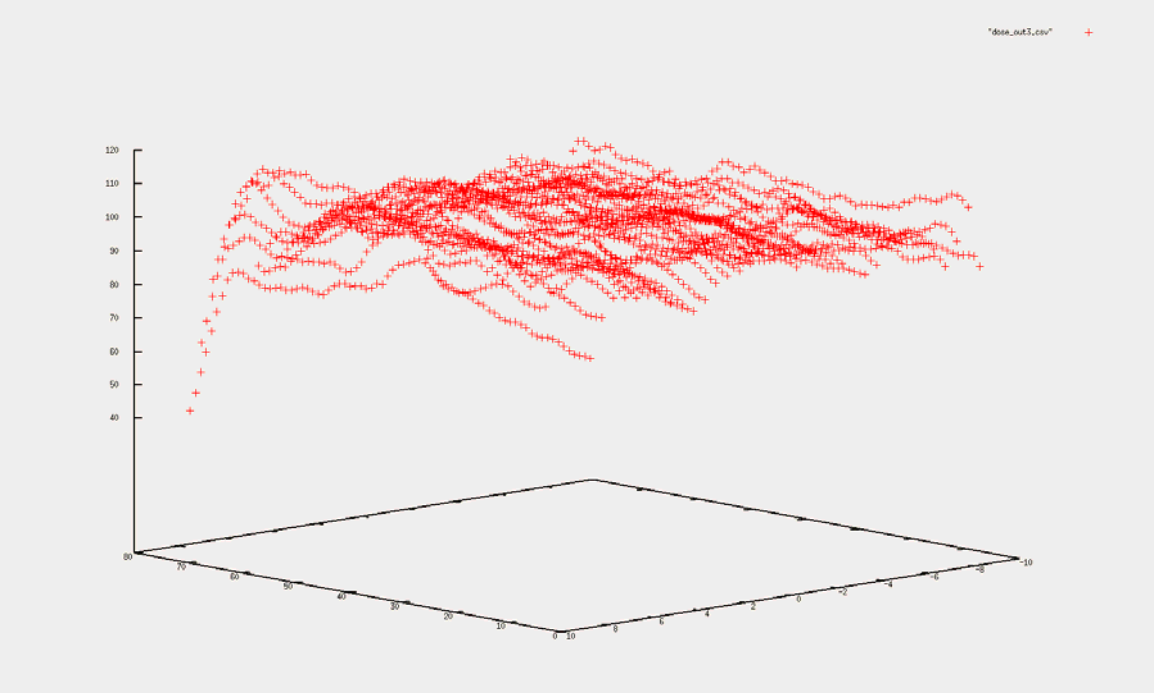

Figure 8: Dose uniformity surface map. Each dose line represents the dose in an axial plane of the phantom. The first two dose lines represent the dose closest to the upper border of the treatment surface. This area, close to the edge of the treated chest wall, represents an area where additional evaluation of the treatment planning code will be required.

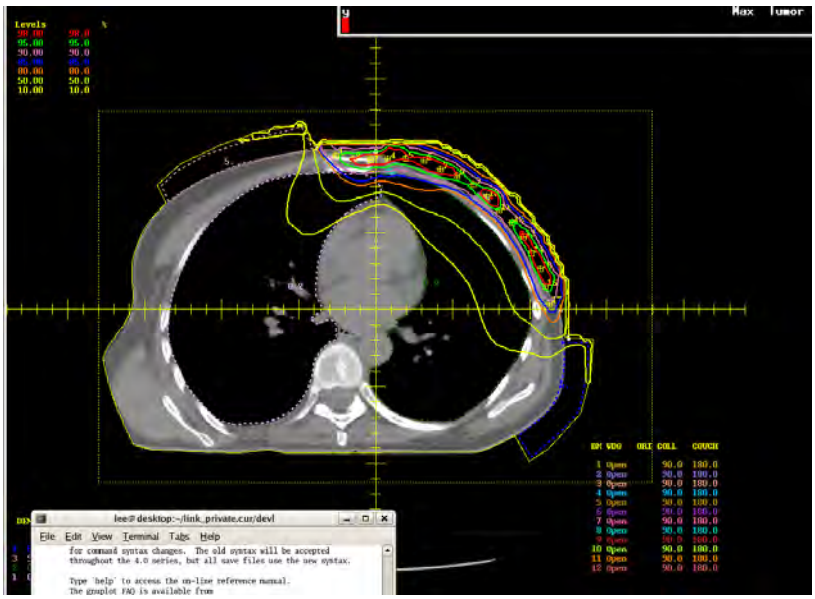

Figure 9: Electron arc therapy dose distribution calculated in central axis plane. Bolus has been added to the post-mastectomy chest wall in order to minimize dose to underlying lung. 6 MeV electrons are applied to the arc since the chest wall is so thin. In the following panels, isodose distributions are displayed for planes +/-4 cm and +/- 8 cm from the central axis. Superposition of these planes demonstrates the change in thoracic thickness in the superior/inferior direction.

Calculation plane +4cm above central axis plane.

Calculation plane 4 cm below central axis plane.

Calculation plane 8 cm above central axis plane.

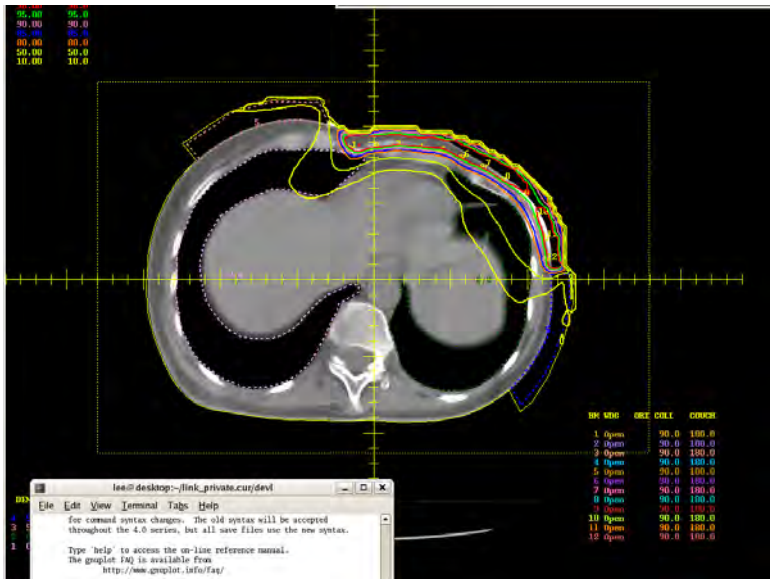

Calculation plane 8 cm below central axis plane.

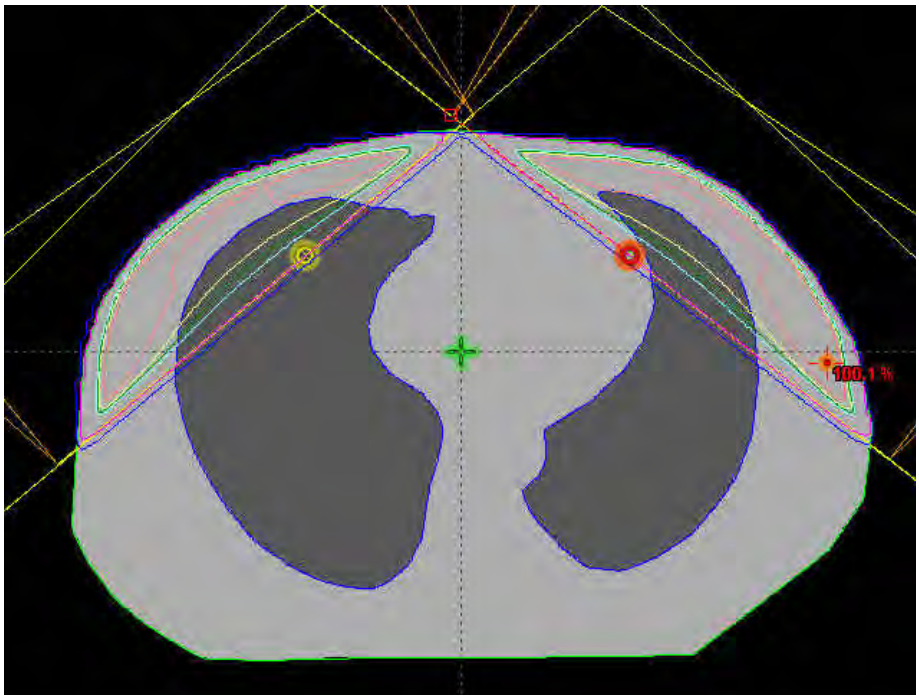

Figure 10: Bilateral post-mastectomy chest wall. Transverse view through thorax. Treated using tangent photons. Note the variation in dose at the junction of the two tangent photon pairs compared to the rest of the chest wall. Compare to the following illustration.

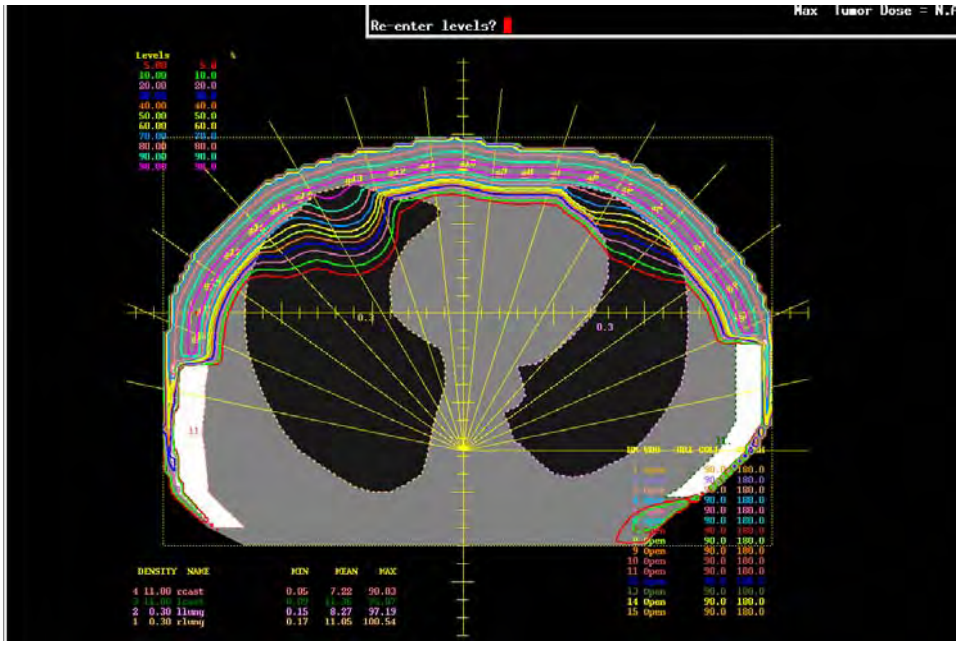

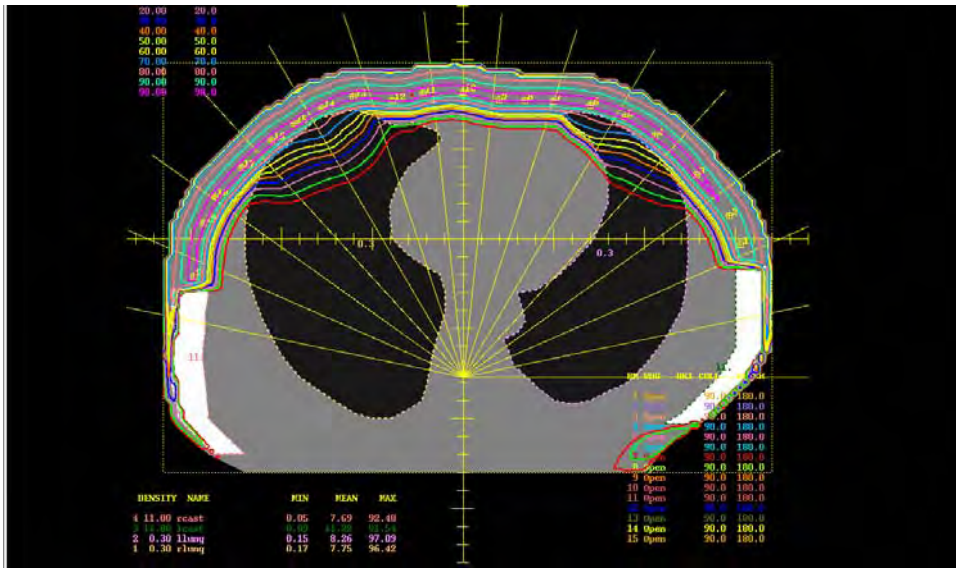

Figure 11: Bilateral post-mastectomy chest wall. Transverse view through thorax. Treated using dynamic electron arc therapy. The arc is divided into multiple arc segments; the Monitor Units per degree is adjusted in each arc segment so the dose across the entire arc is uniform. This eliminates the hot spot/cold spot seen in the bilateral tangent photon treatment plan.

Note that a section of the right chest wall is thin enough that a significant local dose to the lung is seen. Adding bolus to the external chest wall, thereby increasing the effective depth penetrated by electrons before reaching the lung, minimizes this dose.

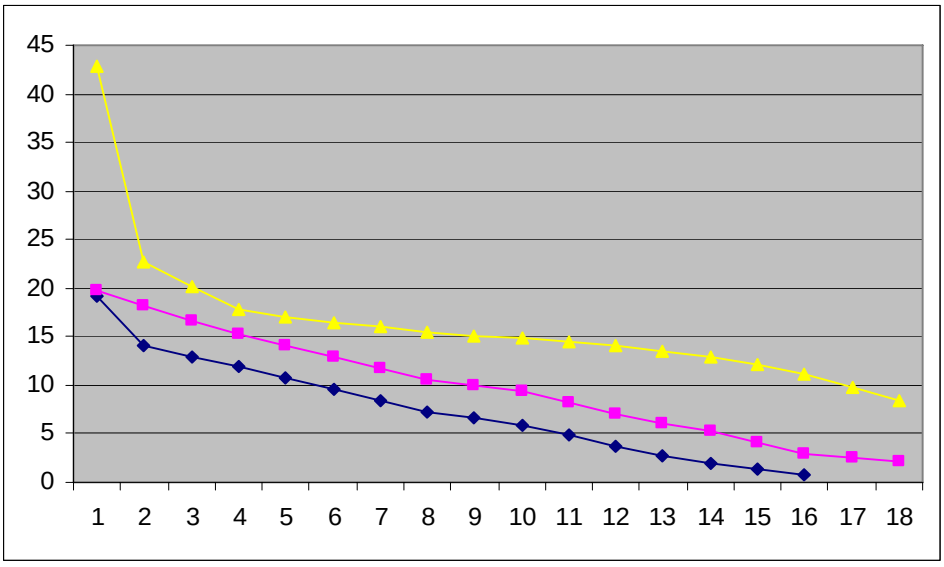

Figure 12: Dose-Volume-Histogram comparing dose to the right lung from tangent photons (top); electron arc without added bolus (middle); and electron arc with added bolus (lowest curve). Y-Axis represents % of right lung receiving a given dose; X-Axis represents doses from 5% (point 1) to 90% (point 18). Clearly, the bilateral arc with proper bolus significantly reduces dose to the lung.

KEY RESEARCH ACCOMPLISHMENTS

- Validation of Monte Carlo electron dose calculations for photon MLC
- Validation of electron Monte Carlo generated beam profiles
- Validation of electron Monte Carlo generated Relative Output Factors
- Validation of dynamic field edge enhancement to eliminate tertiary casting
- Validation of efficacy of photon MLC to define electron arc fields
- Validation of optimization techniques to define MLC shapes vs. angle

REPORTABLE OUTCOMES

Oral Presentations

D. Leavitt, December 2002, "Electron Arc Therapy: Once More with Feeling," M.D. Anderson Cancer Center Visiting Professor, Houston, TX.

D. Leavitt, January 2003, "3-Dimensional Electron Dose Calculations," RAHD Users Conference, Salt Lake City, UT.

D. Leavitt, May 2003, "Heterogeneity Corrections in IMRT Dose Calculations," National Meeting of American Association of Medical Dosimetrists, Providence, RI.

D. Leavitt, June 2003, "Electron Field Shaping using Multi-leaf Collimators," Varian Treatment Planning Conference, Las Vegas, NEV.

D. Leavitt, October 2003, "Electron Arc Therapy Dose Calculations using Monte Carlo," ASTRO National Meeting, Salt Lake City, UT.

D. Leavitt, October 2003, "Heterogeneity Effects in Dose Calculations," ASRT National Meeting, Salt Lake City, UT.

D. Leavitt, May 2005, "Enabling Requirements for Electron Arc Therapy," Varian Engineering Research Conference, Palo Alto, CA.

D. Leavitt, June 2005, "Review of Clinical Electron Dosimetry," National Meeting of American Association of Medical Dosimetrists, San Diego, CA.

D. Leavitt, June 2005, "Research Projects Using Electrons," National Meeting of American Association of Medical Dosimetrists, San Diego, CA.

Published Manuscripts

Hazard L, Miercort C, Gaffney D, Leavitt D, Stewart JR. 2004 Local-regional radiation therapy after breast reconstruction: what is the appropriate target volume? A case-control study of patients treated with electron arc radiotherapy and review of the literature. **Am J Clin Oncol** 27:555-64.

CONCLUSIONS

This project has demonstrated that dynamic Intensity Modulated Electron Radiotherapy, as expressed in Electron Arc Therapy, provides a unique tool for treatment of the post-mastectomy chest wall. The importance of accurate three-dimensional dose calculation models to determine required shapes of the Multi-Leaf Collimator at each increment of the arc has been demonstrated, particularly relating to the changing shape of the chest wall in the cephalo-caudal direction. The calculations, even with an array of some 32 processors, are prohibitively time consuming and will require more work to create a time-efficient calculation model. As presently configured, a complete recalculation is required if only a single MLC shape is changed. This inefficiency is embedded deeply in the code and would require a major rewrite to overcome. Similarly, no efficient optimization algorithm could be developed for this project; therefore, a "gross optimization" that would get the MLC shapes approximately right is followed by an interative optimization which slowly converges.

We have demonstrated that the secondary and tertiary collimation system employed in earlier electron arc therapy work can be replaced by the photon MLC for field shaping, and by dynamic field

edge definition for delineation of the treatment surface. These techniques require further work before they are ready for clinical implementation.

Finally,we have demonstrated successfully the entire dynamic electron arc therapy process, but only in "Service Mode." It will require a major commitment from the radiotherapy equipment manufacturer to enable these features in a clinical mode that would open up this process to the general radiotherapy community.

"So What Section:" Radiation treatment through field abutment lines, as well as dose to normal and critical structures adjacent to the desired treatment volume, remain perplexing problems of radiotherapy. Electron arc therapy provides a unique solution to these problems, and could fill a unique niche on complicated treatments such as bilateral post-mastectomy chest wall treatment. Continuing work must be done to fine a practical, implementable solution to this problem.

REFERENCES - None

APPENDICES - None